Vladimír Janovský
Numerical analysis of a lumped parameter friction model

In: Jan Brandts and Sergey Korotov and Michal Křížek and Karel Segeth and Jakub Šístek and Tomáš Vejchodský (eds.): Application of Mathematics 2015, In honor of the birthday anniversaries of Ivo Babuška (90), Milan Práger (85), and Emil Vitásek (85), Proceedings. Prague, November 18-21, 2015. Institute of Mathematics CAS, Prague, 2015. pp. 63–76.

Persistent URL: http://dml.cz/dmlcz/702965

Conference Applications of Mathematics 2015, in honor of the birthday anniversaries of Ivo Babuška (90), Milan Práger (85), and Emil Vitásek (85)
J. Brandts, S. Korotov, M. Křížek, K. Segeth, J. Šístek, T. Vejchodský (Eds.)
Institute of Mathematics CAS, Prague 2015

NUMERICAL ANALYSIS OF A LUMPED PARAMETER FRICTION MODEL

Vladimír Janovský

Department of Numerical Mathematics, Charles University, Prague,
Sokolovská 83, 186 75 Prague 8, Czech Republic
janovsky@karlin.mff.cuni.cz

Abstract: We consider a contact problem of planar elastic bodies. We adopt Coulomb friction as (an implicitly defined) constitutive law. We will investigate highly simplified lumped parameter models where the contact boundary consists of just one point. In particular, we consider the relevant *static* and *dynamic* problems. We are interested in numerical solution of both problems. Even though the static and dynamic problems are qualitatively different, they can be solved by similar piecewise-smooth *continuation* techniques. We will discuss possible generalizations in order to tackle more complex structures.

Keywords: lumped parameter systems, nonlinear vibrations, Filippov systems, Coulomb friction, impact mechanics

MSC: 65P40, 37M05, 74H15

1. Introduction

Let us consider elastic two-dimensional bodies in mutual contact. The relevant mathematical description consists in modeling of both non-penetration conditions and a friction law. The widely accepted Coulomb friction law represents a serious mathematical and numerical problem. We adopt a discretization via (mixed) Finite Element Method (FEM). The key parameters are degrees of freedom and the number of nodes on the contact boundary. The problems depend on a positive parameter called friction coefficient $\mathcal{F}$.

We have in mind numerical solution of both

1. the *static*, parameter dependent contact problems with Coulomb friction, see e.g. [7, 6, 4, 11, 5],
2. the *dynamic* (i.e. time dependent) contact problems with a friction, see e.g. [9] and with Coulomb friction, [10].

The dynamic solvers use time-stepping schemes (with a fixed stepsize). As a rule, the schemes have to be stabilized. The above authors advocate the stabilization via a *mass redistribution*.

In this contribution we consider a case-study problem with just *one point* on the contact boundary. We analyze both static and dynamic formulations, see [7] and [10]. You may think of toy-problems (lumped parameter models) which reflect the reality qualitatively.

The plan is as follows: In Section 2, we consider the static problem (both the case-study and the example of a real structure). The problem is parameter-dependent in order to model a continuous evolution. The natural numerical tools are continuation (path-following) techniques. The underlying message is: If we learn to solve the toy-problem we get important clues for solving large scale problems. In Section 3 we formulate the dynamic case-study problem. We discuss two numerical techniques: An event-driven algorithm (Section 4) and a time-stepping algorithm (Section 5). In Conclusions (Section 6), we hint at the fact that continuation techniques (Section 2) and, because time is also a parameter, event-driven algorithms and time-stepping algorithms (Section 4 and Section 5) are closely related.

2. The static problem

As a case study, we consider a *static* finite element model of Coulomb friction with one contact point, see [7]: Find $(u_\nu, u_\tau, \lambda_\nu, \lambda_\tau)^T \in \mathbb{R}^4$

$$\left\{\begin{array}{rcl} bu_\nu - cu_\tau - f_\nu - \lambda_\nu &=& 0\,, \\ -cu_\nu + bu_\tau - f_\tau - \lambda_\tau &=& 0\,, \\ \lambda_\nu - P_{(-\infty,0]}(\lambda_\nu - ru_\nu) &=& 0\,, \\ \lambda_\tau - P_{[-\mathcal{F}|\lambda_\nu|,\mathcal{F}|\lambda_\nu|]}(\lambda_\tau - ru_\tau) &=& 0\,. \end{array}\right. \tag{1}$$

Parameters of the model are as follows: The nonnegative friction coefficient $\mathcal{F}$, and the stiffness matrix $\mathbf{A}$,

$$\mathbf{A} = \begin{bmatrix} b & c \\ c & b \end{bmatrix}, \quad b = -\frac{\lambda + 3\nu}{2}\,, \quad c = \frac{\lambda + \nu}{2}\,,$$

where λ and ν are positive parameters (Lamé coefficients). The operators $P_{(-\infty,0]}$ and $P_{[-\mathcal{F}|\lambda_\nu|,\mathcal{F}|\lambda_\nu|]}$ are piecewise linear projectors, see Figure 1. The arguments of both projectors depend on a positive parameter r, that can be arbitrary but fixed.

The system (1) models one linear finite element which rests on a rigid foundation, see Figure 2. The problem is as follows: Given a load $\mathbf{f} = (f_\nu, f_\tau)^\top \in \mathbb{R}^2$, the normal and the tangential *load* components, find

- u_ν and u_τ i.e., the normal and the tangential *displacement*
- λ_ν and λ_τ i.e., the normal and the tangential *stress* components.

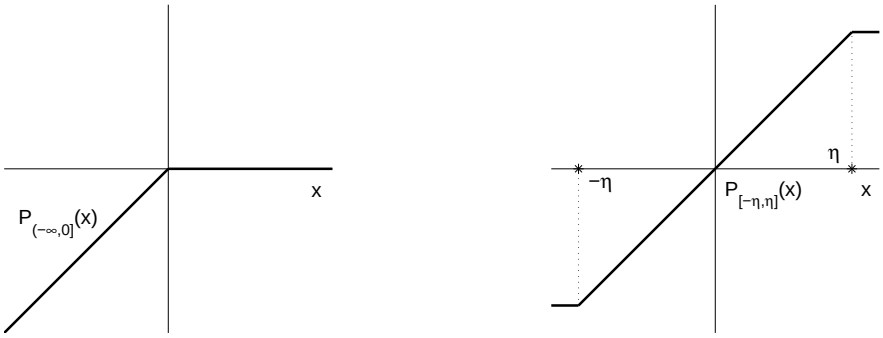

Figure 1: Projectors $x \longmapsto P_{(-\infty,0]}(x)$, $x \longmapsto P_{[-\eta,\eta]}(x)$, $\eta = \mathcal{F}|\lambda_\nu|$.

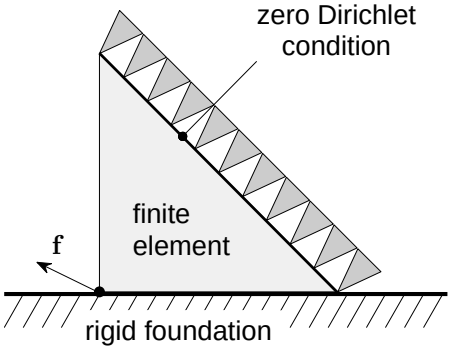

Figure 2: FEM interpretation.

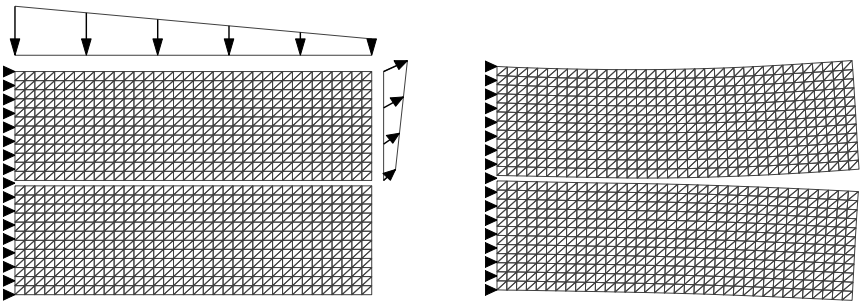

Figure 3: Contact of two elastic bodies Ω^1 (the upper body) and Ω^2, along the contact boundary. The loading is due to the surface traction. Discretization: $n = 1320$ (degrees od freedom), $m = 30$ (number of nodes on the contact boundary). On the right: Resulting deformation.

The system (1) is solvable for any given load $\mathbf{f} \in \mathbb{R}^2$ nevertheless the solution may not be unique. In [6], we proposed path following techniques to find non-unique solutions. The aim was to investigate the model (1) subject to a parameter-dependent force i.e., $\alpha \mapsto f_\nu(\alpha)$ and $\alpha \mapsto f_\tau(\alpha)$. We developed a numerical technique based on *piecewise-smooth continuation*. Starting from this comparatively simple model (1) we generalized the continuation technique for problems of practical interest that involve several thousands elements, see [4, 5]. We also refer to [11] for an alternative approach.

Just to illustrate the technique, we consider the example formulated in [4], see Figure 3. The aim is to investigate dependence of this particular contact problem on the friction coefficient $\mathcal{F}$. The relevant continuation technique is described in [5]. For an illustration of this new technique see Figure 4 and Figure 5. Note that there are three basic contact modes: `no contact`, `contact-stick` and `contact-slip`, see e.g. [6, 4].

3. The dynamic problem

As a case study, we consider a *dynamic* finite element model of Coulomb friction with one contact point, see [10] and Figure 2: We seek for time-dependent functions u_ν, u_τ, λ_ν, $\lambda_\tau : [0, T] \to \mathbb{R}$ such that

$$\mathbf{M} \begin{bmatrix} u_\nu''(t) \\ u_\tau''(t) \end{bmatrix} = \mathbf{A} \begin{bmatrix} u_\nu(t) \\ u_\tau(t) \end{bmatrix} + \begin{bmatrix} f_\nu(t) \\ f_\tau(t) \end{bmatrix} + \begin{bmatrix} \lambda_\nu(t) \\ \lambda_\tau(t) \end{bmatrix} \tag{2}$$

$$-\lambda_\nu(t) \in \mathrm{N}_{\mathbb{R}^1_-}\, u_\nu(t) \tag{3}$$

$$\lambda_\tau(t) \in \mathcal{F}\, \lambda_\nu(t)\, \mathrm{Sign}\, u_\tau'(t) \tag{4}$$

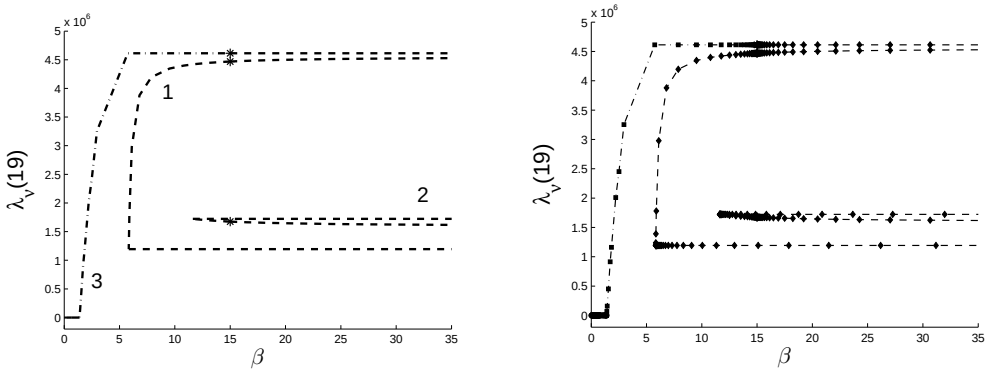

Figure 4: The solution path related to the nodal point No19 consists of three branches. They are initialized by points marked by asterisks. Parameter is $\beta = \mathcal{F}$, the friction coefficient. On the right: An illustrations of the adaptive stepsize refinement of the algorithm. The curves interpretations: solid (no contact), dashed (contact-stick) and dash-dotted (contact-slip).

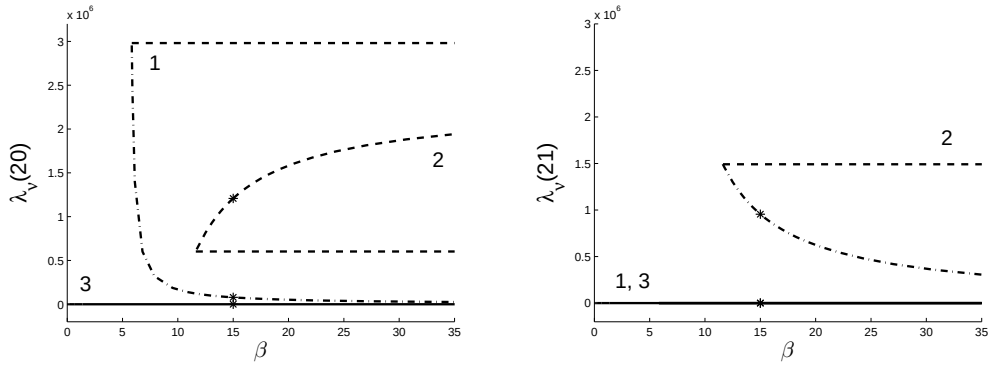

Figure 5: The solution path related to the nodal point No20 (on the left) and the nodal point No21 (on the right). Parameter: $\beta = \mathcal{F}$. The curves interpretations: solid (no contact), dashed (contact-stick) and dash-dotted (contact-slip).

almost everywhere (a.e.) in $[0, T]$. The initial value condition

$$\begin{bmatrix} u_\nu(0) \\ u_\tau(0) \end{bmatrix} = \mathbf{u}^0\,, \quad \begin{bmatrix} u'_\nu(0) \\ u'_\tau(0) \end{bmatrix} = \mathbf{v}^0 \tag{5}$$

is satisfied for any given $\mathbf{u}^0 \in \mathbb{R}^2$, $\mathbf{v}^0 \in \mathbb{R}^2$. The unknowns of the model are

- $u_\nu(t)$ and $u_\tau(t)$ i.e., the normal and the tangential *displacement*
- $\lambda_\nu(t)$ and $\lambda_\tau(t)$ i.e., the normal and the tangential *stress components.*

The data are the given $f_\nu(t)$ and $f_\tau(t)$ i.e., normal and tangential *load* components.

Parameters of the model: The nonnegative friction coefficient $\mathcal{F}$, and the mass and stiffness matrices

$$\mathbf{M} = \begin{bmatrix} a & 0 \\ 0 & a \end{bmatrix}\,, \quad \mathbf{A} = \begin{bmatrix} b & c \\ c & b \end{bmatrix}\,,$$

$$a = \frac{\rho l^2}{12}\,, \quad b = -\frac{\lambda + 3\nu}{2}\,, \quad c = \frac{\lambda + \nu}{2}\,,$$

where ρ, l, λ and ν are positive parameters (the density, the diameter of the element, and two Lamé coefficients).

The symbols Sign and $\mathrm{N}_{\mathbb{R}^1_-}$ denote *multivalued mappings* Sign : $\mathbb{R} \rightrightarrows \mathbb{R}$ and $\mathrm{N}_{\mathbb{R}^1_-} : \mathbb{R} \rightrightarrows \mathbb{R}$ called *signum* and *normal cone*, respectively, see e.g. [1]. We skip formal definitions. Instead, we introduce equivalent formulations via variational inequalities:

The condition (3) is called the *complementarity condition.* It can be interpreted as the `no contact` or the `contact`

$$\begin{cases} \lambda_\nu(t) = 0 & \text{for} \quad u_\nu(t) < 0 \quad \ldots\texttt{no contact} \\ \lambda_\nu(t) \le 0 & \text{for} \quad u_\nu(t) = 0 \quad \ldots\texttt{contact} \end{cases} \tag{6}$$

with the rigid foundation. The condition (4) reads as

$$\begin{cases} \lambda_\tau(t) = \mathcal{F}\,\lambda_\nu(t) & \text{for} \quad u'_\tau(t) > 0 \\ \lambda_\tau(t) = -\mathcal{F}\,\lambda_\nu(t) & \text{for} \quad u'_\tau(t) < 0 \\ |\lambda_\tau(t)| \le -\mathcal{F}\,\lambda_\nu(t) & \text{for} \quad u'_\tau(t) = 0 \end{cases} \tag{7}$$

One can easily conclude that

1. In the case of `no contact` in (6), the condition (7) yields $\lambda_\nu(t) = \lambda_\tau(t) = 0$
2. In the case of `contact` in (6), the condition (7) can be interpreted as

$$\begin{cases} \lambda_\tau(t) = \mathcal{F}\,\lambda_\nu(t) & \text{for} \quad u'_\tau(t) > 0 \quad \ldots\texttt{contact-slip} \\ \lambda_\tau(t) = -\mathcal{F}\,\lambda_\nu(t) & \text{for} \quad u'_\tau(t) < 0 \quad \ldots\texttt{contact-slip} \\ |\lambda_\tau(t)| \le -\mathcal{F}\,\lambda_\nu(t) & \text{for} \quad u'_\tau(t) = 0 \quad \ldots\texttt{contact-stick} \end{cases} \tag{8}$$

The aim is to solve the *initial value problem* (2)–(5). We consider two kinds of algorithms: In Section 4, we introduce an event driven algorithm and in Section 5 we sketch a time-stepping algorithm.

In the following, let us relabel the state variables $x_1 = u_\nu$, $x_2 = u'_\nu$, $x_3 = u_\tau$, $x_4 = u'_\tau$.

4. The event-driven algorithm

The idea is a *dynamical simulation* of the particular solution modes `contact` and `no contact`. They are defined by different systems of ordinary differential equation (i.e., different *vector fields*). Then the solution modes should be concatenated according certain rules (continuity of displacements).

The mode `contact` is modeled as a *Filippov system*, see e.g. [3, 1]. Details can be found in Supplement 7, see the system (12). In this solution mode we have $\lambda_\nu(t) < 0$ on an open time interval $t \ge 0$. It can be shown that $x_1(t) = x_2(t) = 0$, and $\lambda_\nu(t) = -c\,x_3(t) - f_\nu(t) \le 0$. We distinguish two cases:

- If $x_1(t) = x_2(t) = 0$ and $x_4(t) = 0$ then the body is in `contact-stick` regime,
- If $x_1(t) = x_2(t) = 0$ and $x_4(t) \neq 0$ then the body is in `contact-slip` regime.

The dynamical simulation of the contact mode is bases on the *Filippov convex method* and its modifications, [3, 1]. In forthcoming experiments we used the open-source software [12] which is based on the MATLAB ODE suit [15] with an adaptive stepsize.

The mode `no contact` is modeled as two coupled linear oscillators where $\lambda_\nu(t) = \lambda_\tau(t) = 0$, $x_1(t) < 0$ on an open time-interval $t \ge 0$, see Supplement 7, the system (14)&(15).

The coupling of the modes `contact` and `no contact` can be viewed as an *hybrid impact model*, [1]. Why do we call the algorithm an *event-driven* algorithm?

Changing particular modes is linked to the sign-changes of functions $t \mapsto x_1(t)$, $t \mapsto \lambda_\nu(t) \equiv -c\, x_3(t) - f_\nu(t)$ and $t \mapsto x_4(t)$. The MATLAB ODE suit [15] provides an efficient tool called *event location* to localize sign-changes of functionals in space and time.

The given acting force f_ν and f_τ in (2) may be time dependent. In following examples we let the tangential component $f_\tau = f_\tau(t)$ to be periodic and the normal component f_ν to be fixed. We model the action of the craftsman instrument called 'Jack plane'.

Example 4.1 `Contact` *only*
Data*:* $a = 1$, $b = -1.2$, $c = 1$, $\mathcal{F} = 0.4$,
a periodic forcing: $f_\tau(t) = \sin(\omega t)$, $\omega = 1/6$, $f_\nu(t) \equiv f_\nu = 1.3$, *a 'Jack plane' model. The initial condition:* $[0, 0, 0, 0.1]$. *The time-span:* $[0, T]$, $T = 10 \cdot \frac{2\pi}{\omega}$.

The relevant results are shown in Figure 6 and Figure 7. The value of f_ν is sufficiently large and the instrument rests on the foundation for all time.

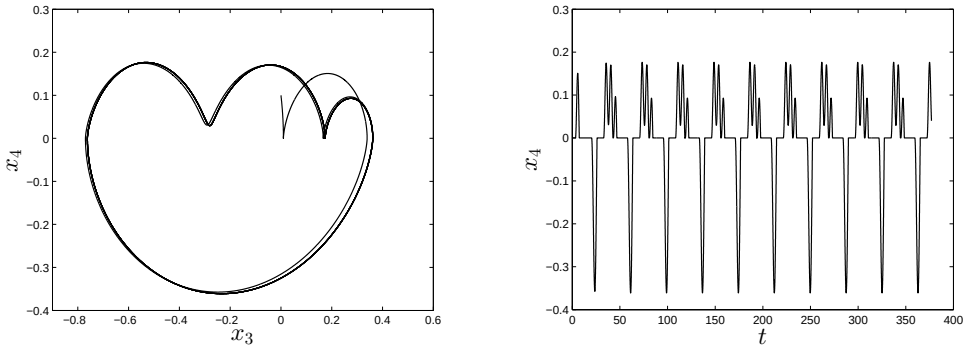

Figure 6: $f_\nu = 1.3$. On the left: A phase plot of x_4 versus x_3. On the right: A plot of x_4 versus time t. Contact regime: If $x_4(t) = 0$ then `contact-stick`. If $x_4(t) \neq 0$ then `contact-slip`.

Example 4.2 *Coupling of the modes* `contact` *and* `no contact`
Data*:* $a = 1$, $b = -1.2$, $c = 1$, $\mathcal{F} = 0.3$,
a periodic forcing: $f_\tau(t) = \sin(\omega t)$, $\omega = 1/6$, $f_\nu(t) \equiv f_\nu = 0.5$, *a 'Jack plane' model. The initial condition:* $[0, 0, 0, 0.1]$. *The time-span:* $[0, T]$, $T = 10 \cdot \frac{2\pi}{\omega}$.

The relevant results are shown in Figure 8 and Figure 9. This time f_ν is small enough and the instrument is lifted from the foundation for particular time periods. The 'Jack plane' is bouncing on the foundation.

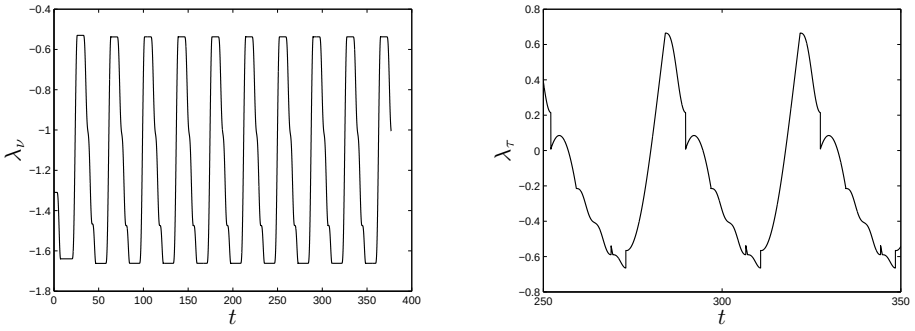

Figure 7: $f_\nu = 1.3$. A plot of λ_ν versus time t. Note that $\lambda_\nu(t) < 0$ characterizes the `contact` mode. On the right: A plot of λ_τ versus time t, a zoom.

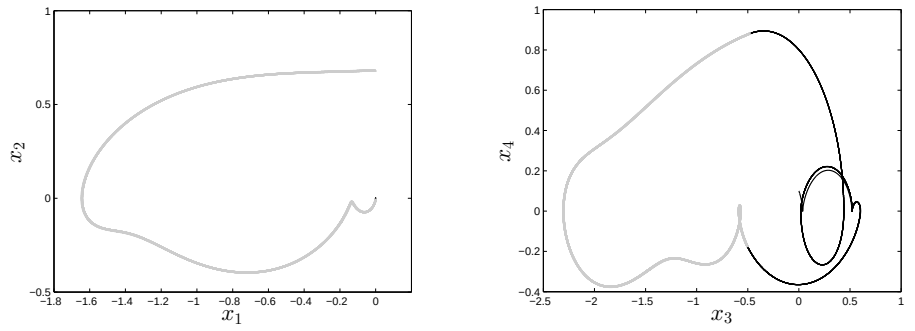

Figure 8: $f_\nu = 0.5$. On the left: A phase plot of x_1 versus x_2. Observe that $x_1 \leq 0$, an impact at $x_1 = 0$. On the right: A phase plot of x_3 versus x_4. Legend: `contact` ... black, `no contact` ... gray.

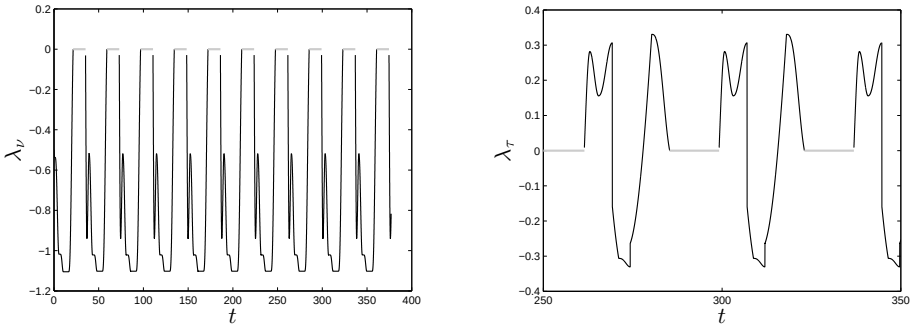

Figure 9: $f_\nu = 0.5$. On the left: A plot of λ_ν versus time t. On the right: A plot of λ_τ versus time t, a zoom. Legend: `contact` ... black, `no contact` ... gray.

5. The time-stepping algorithm

Consider the initial value problem (2)–(5). In [10], there was proposed a natural time discretization of this problem via *mid-point rule* with a fixed stepsize dt. At each time step, the algorithm identifies the solution mode (namely, the options `contact`, `contact − stick` and `contact − slip`) and propose the solution update. The identification is unique provided that the stepsize dt is sufficiently small. (Note that we used the scheme without *mass-redistribution*, [10]). Let us run the mid-point algorithm using the same data as in Example 4.1. We expect qualitatively similar plots as in Figure 6 and Figure 7.

Example 5.3 `Contact` *only, see Example 4.1*
Data*: $a = 1$, $b = -1.2$, $c = 1$, $\mathcal{F} = 0.4$, time increment $dt = 0.001$,*
a periodic forcing: $f_\tau(t) = \sin(\omega t)$, $\omega = 1/6$, $f_\nu(t) \equiv f_\nu = 1.3$, a 'Jack plane' model.
The initial condition: $[0, 0, 0, 0.1]$. The time-span: $[0, T]$, $T = 10 \cdot \frac{2\pi}{\omega}$.

In Figure 10, on the left, there is a plot of initial stages of x_4 computed via the mid-point rule. Note that corresponding zoom in Figure 6, on the right, computed via the event-driven algorithm would look much the same. Remarkable are the run-time differences: 2495.6 seconds (the mid-point rule) vs 2.3 seconds (the event-driven algorithm). The zoom in Figure 10 reveals that the numerical solution oscillates between the stages `contact-slip` and `contact-stick` (see the isolated dots). In that case, the remedy is to guide the solution to remain in regime `contact-stick`. It can be done by adapting slightly the original code in [10] e.g., in case `contact-stick` we set directly $x_4 = 0$. We call the resulting algorithm the *stabilized* mid-point rule. In Figure 11, we plot x_4 versus t computed via stabilized mid-point rule. Due to the setting of Example 5.3, i.e. `contact` only, we have just two competing modes namely `contact-slip` and `contact-stick` depicted by dashed and solid curves. Elapsed time was 64.841882 seconds (stabilized mid-point rule, $0 \le t \le 380$, $dt = 0.001$).

The above stabilization technique can be related to the approach by [2, 14].

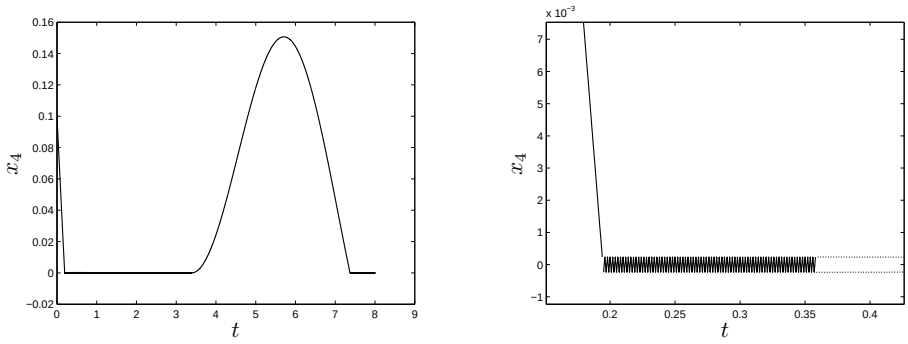

Figure 10: $f_\nu = 1.3$, time increment $dt = 0.001$. On the left: The solution via mid-point rule. A plot of x_4 versus t as $0 \le t \le 8$. On the right: a zoom.

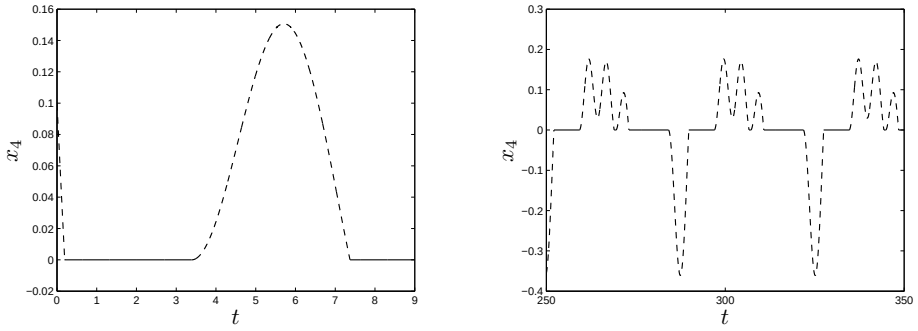

Figure 11: $f_\nu = 1.3$, time increment $dt = 0.001$. The solution via *stabilized* midpoint rule. Legend: `contact-stick` ... solid, `contact-slip` ... dashed curves. On the left: the initial stages $0 \leq t \leq 9$. On the right: The periodic pattern of the limit set, $250 \leq t \leq 350$.

6. Conclusions

We considered simplified models (i.e., lumped parameter models) for both the static, see (1), and the dynamic friction model, see (2)–(5).

The static model (1) is piecewise smooth, parameter dependent. It can be solved by continuation techniques. The dynamic model (2)–(5) is piecewise smooth dynamical system where time t is a parameter. The approaches to numerical solution (the event-driven algorithm in Section 4 and the time-stepping algorithm in Section 5) can be viewed as approximations of discrete time, piecewise-smooth dynamical systems. Both the static and dynamic problems can be solved by similar (continuation) techniques in spite of the fact that both models are qualitatively different. The continuation techniques for solving the static case-study model (1) can be extended to higher dimensions. We hope for such an extension for dynamic contact problems which would deal with structures as in Figure 3.

Comparison of the event-driven algorithm and the time-stepping algorithm: In [8], we compared an event-driven algorithm (based on the software in [12]) and a time-stepping algorithm (based on implicitly defined law of Coulomb friction, [14, 2, 13]) for the Dry-friction model (in 2-D) i.e., the model of a slide fastener. The comparison in [8] argue strongly for an event-driven algorithm:

1. In [12], there is implemented an adaptive stepsize refinement. As a consequence, the solver reduces the computational costs.
2. The solution modes are clearly distinguished and precisely localized (in case of Dry friction we distinguish just $\texttt{contact} - \texttt{slip}$ and $\texttt{contact} - \texttt{stick}$ modes).

Coming back to the algorithms formulated in Section 4 and Section 5, respectively: The event-driven algorithm seems to be superior to the time-stepping algorithm. The argument for this statement is the same as the above. Mind you the

failure in Figure 10, on the left. It can be fixed, see Figure 11. Nevertheless, there is a space for improvements as the mode identification is concerned.

On the other hand, the event-driven algorithm uses built-in MATLAB routines namely, the routines concerning the stepsize control, see [15]. When thinking about possible generalizations of event-driven algorithms in order to deal with real structures as in Figure 3, one has to programm adaptive step refinement or event-location routines himself. In principle, it is possible. In the continuation context, the key algorithms are already developed, see Figure 4, on the right.

7. Supplement: Modelling the modes `contact` and `no contact`

This supplement pertains to Section 4, giving particular details. Basically, we shall follow [8].

7.1. The `contact` mode

Assume that the body is in contact with the rigid foundation at a particular time $t^0 \geq 0$ and on an open non-empty time interval $\mathcal{I}(t^0)$. It means that the equations (2) together with the conditions $\{\lambda_\nu(t) \leq 0\,,\ u_\nu(t) = 0\}$ and (8) are satisfied for $t \in \mathcal{I}(t^0)$.

The system (2) consists of two equations:

$$a u''_\nu(t) = b u_\nu(t) + c u_\tau(t) + f_\nu(t) + \lambda_\nu(t) \tag{9}$$

$$a u''_\tau(t) = c u_\nu(t) + b u_\tau(t) + f_\tau(t) + \lambda_\tau(t) \tag{10}$$

Since $u_\nu(t) = 0$ for all $t \in \mathcal{I}(t_0)$ then $u''_\nu(t) = 0$ for all $t \in \mathcal{I}(t_0)$. The equation (9) reduces to an algebraic constraint:

$$\lambda_\nu(t) = -c\, u_\tau(t) - f_\nu(t)\,, \quad \lambda_\nu(t) \leq 0 \tag{11}$$

for $t \in \mathcal{I}(t^0)$. From (10) and (8), we conclude that

1. If $u'_\tau > 0$ then $\lambda_\tau = \mathcal{F}\lambda_\nu$, see (8). The equations (10)&(11) yield

$$u''_\tau = \frac{b - \mathcal{F}c}{a} u_\tau + \frac{1}{a}\,(f_\tau - \mathcal{F} f_\nu)$$

2. If $u'_\tau < 0$ then $\lambda_\tau = -\mathcal{F}\lambda_\nu$, see (8). Due to the equations (10)&(11)

$$u''_\tau = \frac{b + \mathcal{F}c}{a} u_\tau + \frac{1}{a}\,(f_\tau + \mathcal{F} f_\nu)$$

3. If $u'_\tau = 0$ then $|\lambda_\tau| \leq -\mathcal{F}\lambda_\nu$, see (8). In a spirit of the Filippov convex method [3, 1] we consider the convex combination of the right-hand sides of the above equations

$$u''_\tau = \frac{(1-2\lambda)\,\mathcal{F}c + b}{a}\, u_\tau + \frac{1}{a} f_\tau + \frac{1-2\lambda}{a}\,\mathcal{F} f_\nu\,, \quad \lambda \in [0,1]\ .$$

Let us relabel the state variables $x_1 = u_\nu$, $x_2 = u'_\nu$, $x_3 = u_\tau$ and $x_4 = u'_\tau$. Accordingly, we introduce vector fields $F_1 : \mathbb{R}^5 \to \mathbb{R}^5$ and $F_2 : \mathbb{R}^5 \to \mathbb{R}^5$ as

$$F_1 = \begin{bmatrix} 0 \\ 0 \\ x_4 \\ \dfrac{b - \mathcal{F}c}{a}\, x_3 + \dfrac{1}{a}\,(f_\tau - \mathcal{F} f_\nu) \\ 1 \end{bmatrix}, \quad F_2 = \begin{bmatrix} 0 \\ 0 \\ x_4 \\ \dfrac{b + \mathcal{F}c}{a}\, x_3 + \dfrac{1}{a}\,(f_\tau + \mathcal{F} f_\nu) \\ 1 \end{bmatrix}$$

where $f_\tau = f_\tau(t) = f_\tau(x_5)$, $f_\nu = f_\nu(t) = f_\nu(x_5)$. The vector fields F_1 and F_2 are autonomous (which was the condition to use the ready-made software [12]). Nevertheless, we can recover time t easily.

Moreover, we define the level-set operator $H_{12} : \mathbb{R}^5 \to \mathbb{R}$,

$$H_{12}(x) = x_4\,.$$

The fields F_1 and F_2, respectively, are defined on

$$S_1 = \left\{x \in \mathbb{R}^5 :\, H_{12}(x) > 0\right\} \quad \text{end} \quad S_2 = \left\{x \in \mathbb{R}^5 :\, H_{12}(x) < 0\right\}\,.$$

The set $\Sigma_{12} = \{x \in \mathbb{R}^5 :\, H_{12}(x) = 0\}$ is the discontinuity surface. We consider the Filippov system

$$x' = \begin{cases} F_1(x) & \text{for} \quad x \in S_1 \\ F_2(x) & \text{for} \quad x \in S_2 \end{cases} \tag{12}$$

For a given initial condition $x^0 \in \mathbb{R}^5$, the Filippov's convex method, e.g. [3, 1, 12], gives the solution of the system (12) on a time span for which the body stays in contact with the rigid obstacle i.e.,

$$\lambda_\nu(t) = -c\, x_3(t) - f_\nu(t) \le 0\,.$$

It means that the initial condition $x^0 \in \mathbb{R}^5$ has to satisfy

$$x^0 = \left[0, 0, x^0_3, x^0_4, t^0\right]^\top, \quad -c\, x^0_3(t^0) - f_\nu(t^0) < 0\,. \tag{13}$$

7.2. The `no contact` mode

Recall the original meaning of the state variables $x_1 = u_\nu$, $x_2 = u'_\nu$, $x_3 = u_\tau$ and $x_4 = u'_\tau$. Assume that the body is not in contact with the rigid foundations at a particular time $t^0 \ge 0$ and on an open non-empty time interval $\mathcal{I}(t^0)$. Due to (6) (the option `no contact`) we can claim that $\{\lambda_\nu(t) = 0, u_\nu(t) < 0\}$ for $t \in \mathcal{I}(t_0)$. We

already noted that $\lambda_\nu(t) = \lambda_\tau(t) = 0$ for $t \in \mathcal{I}(t^0)$, as a consequence of (7). Hence, the system (2) reduces to equations

$$au''_\nu(t) = bu_\nu(t) + cu_\tau(t) + f_\nu(t) \tag{14}$$

$$au''_\tau(t) = cu_\nu(t) + bu_\tau(t) + f_\tau(t) \tag{15}$$

for $t \in \mathcal{I}(t^0)$ provided that $u_\nu(t) < 0$. We formulate (14)&(15) as an autonomous system adding an extra equation $t' = 1$. Coming back to the variable $x \in \mathbb{R}^5$ we introduce the vector field $F_3 : \mathbb{R}^5 \to \mathbb{R}^5$ as

$$F_3 = \begin{bmatrix} x_2 \\ \frac{b}{a}x_1 + \frac{c}{a}x_3 + \frac{1}{a}f_\nu(x_5) \\ x_4 \\ \frac{c}{a}x_1 + \frac{b}{a}x_3 + \frac{1}{a}f_\tau(x_5) \\ 1 \end{bmatrix} .$$

The field F_3 is defined on

$$S_3 = \left\{ x \in \mathbb{R}^5 : \, x_1 < 0 \right\} .$$

Acknowledgements

This work was supported by the grant GAČR P201/12/0671.

References

[1] di Bernardo, M., Budd, C. J., Champneys, A. R., and Kowalczyk, P.: *Piecewise-smooth Dynamical Systems. Theory and Applications.* Springer Verlag, New York, 2008.

[2] Darbha, S., Nakshatrala, K., and Rajagopal, K.: On the vibrations of lumped parameter systems governed by differential-algebraic equations. Journal of the Franklin Institute **347** (2010), 87–101.

[3] Filippov, A. F.: *Differential equations with discontinuous righthand sides.* Kluwer Academic Publishers, Dordrecht, 1988.

[4] Haslinger, J., Janovský, V., and Kučera, R.: Path-following the static contact problem with coulomb friction. In: J. Brandts, S. Korotov, M. Křížek, J. Šístek, and T. Vejchodský (Eds.), *Proceedings of the International Conference Application of Mathematics 2013, Prague, May 15-17, 2013*, pp. 104–116. Institute of Mathematics, Academy of Sciences of the Czech Republic, 2013.

[5] Haslinger, J., Janovský, V., Kučera, R., and Motyčková, K.: Nonsmooth continuation of parameter dependent static contact problems with Coulomb friction. Mathematics and Computers in Simulation (submitted).

[6] Haslinger, J., Janovský, V., and Ligurský, T.: Qualitative analysis of solutions to discrete static contact problems with Coulomb friction. Comp. Meth. Appl. Mech. Engrg. **205–208** (2012), 149–161.

[7] Hild, P. and Renard, Y.: Local uniqueness and continuation of solutions for the discrete Coulomb friction problem in elastostatics. Quart. Appl. Math. **63** (2005), 553–573.

[8] Janovský, V.: Lumped parameter friction models. In: *Proceedings of 4th Scientific Colloquium, Prague, June 24-26, 2014*, pp. 132–149. Institute of Chemical Technology, Czech Republic, 2014.

[9] Khenous, H., Laborde, P., and Renard, I.: Mass redistribution method for finite element contact problems in elastodynamics. Eur. J. Mech., A/Solids **27** (2008), 918–932.

[10] Ligurský, T. and Renard, I.: A well-posed semi-discretization of elastodynamic contact problems with friction. Quart. J. Mech. Appl. Math. **64** (2011), 215–238.

[11] Ligurský, T. and Renard, I.: A continuation problem for computing solutions of discretised evolution problems with application to plane quasi-static contact problems with friction. Comp. Meth. Appl. Mech. Engrg. **280** (2014), 222–262.

[12] Piiroinen, P. and Kuzetsov, Y. A.: An event-driven method to simulate Filippov systems with accurate computing of sliding motions. ACM Transactions on Mathematical Software **34** (2008).

[13] Pražák, D. and Rajagopal, K.: Mechanical oscillators described by a system of differencial-algebraic equation. Appl. Math. **57** (2012), 129–142.

[14] Rajagopal, K.: A generalized framework for studying vibrations of lumped parameter systems. Mech. Res. Comm. **37** (2010), 463–466.

[15] Shampine, L. and Reichelt, M.: The matlab ode suit. SIAM J. Sci. Comput. **18** (1997), 1–19.